# Procedures for the Study of the Flexible-Disk to Head Interface

The response of a rotating flexible disk interacting with a read-write head is analyzed. The disk deflection due to an arbitrary distributed normal pressure is coupled with the Reynolds lubrication equation for the disk-to-head air bearing. Procedures which considerably reduce the computation time necessary for obtaining a converged solution are described. A parameter study is then discussed and its results presented.

#### Introduction

Flexible disks, used extensively as a means of magnetically storing digital information, have a typical configuration consisting of a thin mylar disk rotating in close proximity to a stationary and rigid base plate. Due to the hydrodynamics involved, the presence of the base plate beneath the disk causes the disk to deform downward toward the plate, resulting in a stabilizing effect on its transverse motion. Protruding through a radial slot in the base plate is a magnetic read-write head which penetrates upward toward the disk. This causes a thin air bearing to be induced between the disk and head which locally stabilizes the disk deflections. The problem is that in order to achieve high data bit density it is desirable to maintain an extremely thin air bearing. However, if the resulting "flying height" is too small, intermittent contact or collapse of the air bearing can occur, resulting in excessive disk wear.

The first analysis directed toward the mechanics of this problem was made by Pelech and Shapiro [1]. They determined the deformed shape of the spinning disk due to the presence of the base plate without a magnetic head. This axisymmetric problem was solved by coupling the mechanics of the flexible disk, as described by thin membrane theory, with the fluid dynamics of the air film separating the disk from the base plate. The problem of a stationary nonaxisymmetric load distribution acting on a rotating disk was studied by Benson and Bogy [2]. They found that the membrane operator was singular so that the effect of bending stiffness, no matter how small, still had to be included in the problem formulation. Chang [3]

solved this problem using plate theory in which bending stiffness was included. Some further refinements of the method were made by Greenberg and Chang [4]. Then Greenberg [5] coupled the procedure of [4] with the Reynolds equation describing the fluid mechanics of the diskto-head air bearing. In [6], Greenberg uses a similar coupling procedure to solve a head-tape interaction problem. Adams [7] includes the effect of the base plate and foundation stiffness. While the methods described in the preceding papers provide a procedure for solving the flexible disk problem, convergence problems exist and these methods are impractical to use for a parameter study because of the excessive amount of computation time necessary. Even for the simplest case, that of a spherical contour head, over ten hours of CPU time on an IBM 370/ 168 is necessary in order to obtain a converged solution. In order to study the effects of such parameters as head contour, head position, penetration, and head dimensions, it is necessary to solve the problem much more rapidly. It is the purpose of this paper to show how this can be accomplished and to present the results obtained in that manner.

## **Problem formulation**

The problem considered requires the simultaneous solution of an elasticity problem and a fluid mechanics problem. The fourth-order partial differential equation relating the unknown transverse deflection  $w(r, \theta, t)$  of the flexible disk to the unknown pressure  $q(r, \theta, t)$  which acts in the air bearing between the disk and the read-write head (Fig. 1) is given by

Copyright 1980 by International Business Machines Corporation. Copying is permitted without payment of royalty provided that (1) each reproduction is done without alteration and (2) the *Journal* reference and IBM copyright notice are included on the first page. The title and abstract may be used without further permission in computer-based and other information-service systems. Permission to republish other excerpts should be obtained from the Editor.

$$\rho \frac{\partial^2 w}{\partial t^2} = \frac{1}{r} \frac{\partial}{\partial r} \left( \sigma_r(r) r \frac{\partial w}{\partial r} \right) + \sigma_{\theta}(r) \frac{1}{r^2} \frac{\partial^2 w}{\partial \theta^2} - \frac{D}{h} \nabla^4 w$$
$$- \frac{K}{h} w - \frac{C}{h} \frac{\partial w}{\partial t} + \frac{1}{h} q(r, \theta, t), \tag{1}$$

where

 $\rho = \text{mass per unit volume (kg/m}^3),$ 

h =thickness of the disk (m),

$$D = \frac{Eh^3}{12(1 - \nu^2)}$$
 (N-m),

 $\nu$  = Poisson's ratio.

 $E = \text{Young's elastic modulus } (\text{N/m}^2),$ 

K = elastic foundation constant (N/m<sup>3</sup>),

 $C = \text{damping constant } (N-s/m^3).$ 

 $\omega$  = angular velocity of the disk (rad/s),

a = inner radius of the disk (m),

b =outer radius of the disk (m),

 $\sigma_r$ ,  $\sigma_\theta$  = in-plane stresses (N/m<sup>2</sup>), with

$$\begin{split} \sigma_r &= \frac{\rho \omega^2}{8} \ (\ 3 + \nu)(b^2 - r^2) \bigg[ 1 + \frac{1 - \nu}{3 + \nu} \, \gamma a^2 / r^2 \bigg], \\ \sigma_\theta &= \frac{\rho \omega^2}{8} \ \bigg[ (1 + \nu)(a^2 + \gamma b^2) - (1 + 3\nu) r^2 \\ &\qquad - (1 - \nu) \gamma \, \frac{a^2 b^2}{r^2} \bigg], \text{ and} \\ \gamma &= \frac{(3 + \nu)b^2 - (1 + \nu)a^2}{(1 + \nu)b^2 + (1 - \nu)a^2} \, . \end{split}$$

Note that the disk-to-head air-bearing pressure is given by  $q(r, \theta, t)$ , whereas the air pressure due to the presence of the base plate is accounted for by the term K.

The boundary conditions are that the disk is clamped at its inner radius

$$w(r, \theta, t)\big|_{r=a} = 0, \tag{2}$$

$$\frac{\partial}{\partial r} w(r, \theta, t)|_{r=a} = 0, \tag{3}$$

and free at its outer radius

$$\frac{\partial^2 w}{\partial r^2} + \nu \left( \frac{1}{r} \frac{\partial w}{\partial r} + \frac{1}{r^2} \frac{\partial^2 w}{\partial \theta^2} \right) \Big|_{r=b} = 0, \tag{4}$$

$$\frac{\partial}{\partial r} \left( \frac{\partial^2 w}{\partial r^2} + \frac{1}{r} \frac{\partial w}{\partial r} + \frac{1}{r^2} \frac{\partial^2 w}{\partial \theta^2} \right) + \frac{1 - \nu}{r^2} \frac{\partial^2}{\partial \theta^2} \left( \frac{\partial w}{\partial r} - \frac{w}{r} \right) \Big|_{r=b} = 0.$$
(5)

In (1) the first term is from inertia, the next two come from in-plane membrane stresses due to rotation, the fourth is from bending stiffness, the fifth term is an elastic foundation parameter, the sixth is from damping, and the last term is the loading from the air bearing.

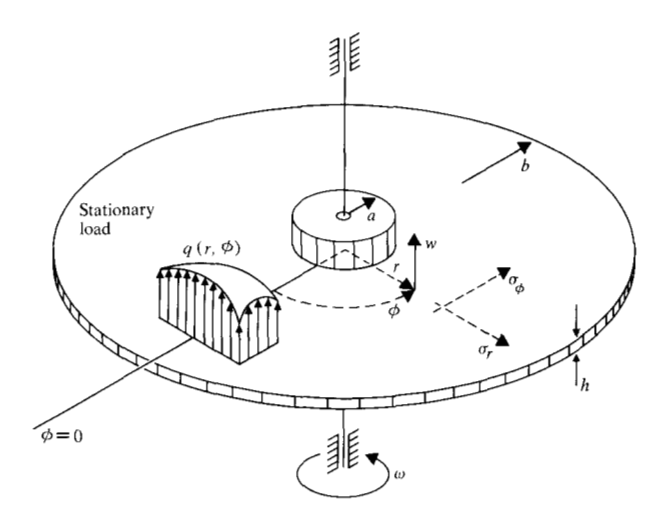


**Figure 1** Rotating flexible disk penetrated by a read-write head (taken from Reference [7], copyright 1980 by the ASME; reprinted with permission). (Note:  $\theta$  and  $\phi$  are the body-fixed and space-fixed angular coordinates, respectively.)

Proceeding as in [3], we transfer from the body-fixed coordinates  $(r, \theta)$  to the space-fixed system  $(r, \phi)$ . Considering steady-state solutions this becomes

$$\phi = \theta + \omega t. \tag{6}$$

Then, expanding both the pressure load and the transverse deflection as a Fourier series in the circumferential direction.

$$q(r, \phi) = \sum_{p=-\infty}^{\infty} Q_p(r)e^{ip\phi}, \tag{7}$$

$$Q_p(r) = \frac{1}{2\pi} \int_0^{2\pi} q(r, \phi) e^{-ip\phi} d\phi,$$
 (8)

$$w(r, \phi) = \sum_{p=-\infty}^{\infty} R_p(r)e^{ip\phi}$$
 (9)

leads to an infinite set of fourth-order ordinary differential equations for the Fourier components of the deflection

$$L_p R_p(r) = \frac{1}{D} Q_p(r), \qquad p = -\infty \text{ to } \infty,$$
 (10)

with

$$\begin{split} L_p &\equiv \frac{d^4}{dr^4} + \frac{2}{r} \, \frac{d^3}{dr^3} - \frac{1}{r^2} \bigg[ 1 + 2p^2 + \frac{h}{D} \, r^2 \sigma_r(r) \bigg] \, \frac{d^2}{dr^2} \\ &+ \frac{1}{r^3} \, \bigg\{ 1 + 2p^2 - \frac{h}{D} \, r^2 \frac{d}{dr} \, \big[ r \sigma_r(r) \big] \bigg\} \, \frac{d}{dr} \\ &+ \frac{1}{r^4} \, \bigg\{ \, p^4 - 4p^2 + \frac{h}{D} \, r^2 \big[ \sigma_{\phi}(r) - \rho \omega^2 r^2 \big] p^2 \\ &+ \frac{K}{D} \, r^4 + i \, \frac{\omega c}{D} \, r^4 p \bigg\}. \end{split}$$

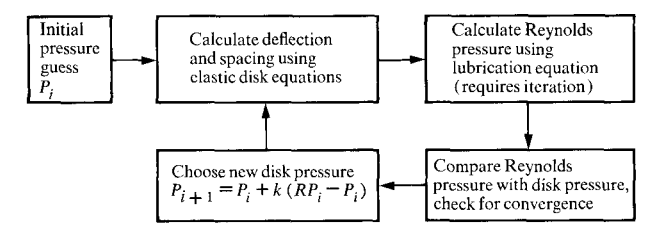


Figure 2 Coupling scheme. (Note: k is the relaxation factor and  $RP_i$  is the Reynolds pressure.)

Each of these ordinary differential equations is solved using a five-point finite difference scheme [8], subject to boundary conditions obtained from (2)-(5) with (9). The disk deflection at any point is given by

$$w(r, \phi) = X_0(r) + 2 \sum_{p=1}^{\infty} [X_p(r) \cos(p\phi) - Y_p(r) \sin(p\phi)],$$
 (11)

where

$$R_{p}(r) = X_{p}(r) + iY_{p}(r).$$

The method just outlined gives us a procedure for determining the disk deflection for an arbitrary prescribed pressure.

Considering slip flow due to molecular effects, we write the steady-state Reynolds equation for gas-lubricated bearings in rectangular coordinates, nondimensionalized with respect to head length, as [9, 10]

$$\frac{\partial}{\partial \xi} \left[ q H^3 \frac{\partial q}{\partial \xi} \right] + \frac{\partial}{\partial \eta} \left[ q H^3 \frac{\partial q}{\partial \eta} \right] 
+ 6m \left[ \frac{\partial}{\partial \xi} \left[ H^2 \frac{\partial q}{\partial \xi} \right] + \frac{\partial}{\partial \eta} \left[ H^2 \frac{\partial q}{\partial \eta} \right] \right] 
= \Lambda \frac{\partial}{\partial \xi} \left[ q H \right],$$
(12)

subject to atmospheric boundary conditions along the edges of the head. In (12), q and H are the normalized pressure and spacing, respectively, m is the Knudsen number (ratio of molecular mean free path to minimum spacing), and  $\Lambda$  is the gas bearing number. The spacing between the disk and head is the difference between the disk deflection, obtained from the disk dynamics equations, and the head contour, which is fixed. The spacing is then prescribed in (12), which is solved for the pressure using finite differences along with Gauss-Seidel relaxation, and requires a 51  $\times$  51 grid in the air bearing.

The elastohydrodynamic system describing the interaction between the read-write head and the flexible disk requires the simultaneous solution of (1) and (12). Unfor-

tunately, a direct analytic combination of the two equations would be impractical. The method used in [5] is outlined in Fig. 2. As previously noted in the Introduction, the solution obtained using this procedure takes over ten hours of CPU time on a 370/168 system for the simplest head geometry—that of a spherical head, and in order for the solution to be usable, a quicker numerical procedure is necessary.

## Improved numerical method

The solution of the coupled elastohydrodynamic problem requires the solutions of both (1) and (12) for each iteration (Fig. 2). Since the Reynolds equation is nonlinear, its solution also requires an iterative procedure. It has been found that, in order for convergence to be achieved, an extremely accurate solution of the lubrication equation is necessary (the pressure residual must be of order  $10^{-8}$ ). Since the solution of (12) requires an initial pressure guess followed by iteration until convergence is obtained, it follows that an excellent pressure guess for the Reynolds equation solution can significantly reduce computational time. This initial pressure distribution is found by extrapolation of the last two Reynolds equation solutions and reduces computational time for the lubrication equation by an average factor of three. The time savings are particularly significant when the coupled equations are near convergence, since the Reynolds equation solution does not change appreciably from one iteration to the next.

It has also been found that an extremely accurate solution of the elasticity equations is necessary in order for a converged solution to be obtained. In general this requires about 200 Fourier modes and 500 radial grid points. The main reason for this accuracy problem is that the disk-to-head spacing is the difference between the disk deflection and the head contour. Since these two values are nearly equal, small errors in the elasticity equations can lead to significant errors in the spacing.

The solution of our elasticity equations requires solving linear equations with a given number of modes and grid points. Since solution of linear equations requires a fixed number of operations, it might seem that a substantial reduction of computation time would not be possible. However, we will show how to take advantage of the linearity of the elasticity equations in order to develop a method which eliminates the need for a complete solution during each iteration. Let  $\Delta P$  be the change in disk pressure from one step to the next, and let  $\Delta w$  be the corresponding change in disk deflection (which is also equal to the change in spacing). Then (1) can be solved with the pressure increment  $\Delta P$  prescribed, which yields the deflection increment  $\Delta w$ . The advantage is that  $\Delta P$  is generally much smaller than P, so that these equations can be

solved with much less accuracy. The spacing increment  $\Delta w$  is then added to the previous value of the spacing. In order to avoid a possible accumulation of errors, a calculation with the actual value of P is made after every five iterations. Additional time can be saved by starting with fewer modes and grid points, then gradually increasing them as the disk-to-head spacing decreases. These methods result in reducing the computation time by almost a factor of two.

The procedures described thus far are effective because they reduce the time required to solve each of the two equations (1) and (12). We now focus our attention on the scheme used to couple these two problems. As already mentioned, a direct analytical combination of the two equations would be desirable, yet is impracticable to obtain. The coupling scheme (Fig. 2) represents a weak combination of the two systems as it requires the complete solution of each problem separately. The method developed here involves a direct combination of both equations which can be most readily accomplished when they are written in numerical form. Let us symbolically represent the elasticity solution in numerical form by

$$w(r_i, \phi_j) = L[P(r_i, \phi_j)], \tag{13}$$

where  $L[\ ]$  is the linear operator representing the solution procedure obtained using Fourier series along with finite differences. The Reynolds equation of lubrication in numerical form can be written as

$$R[P(r_i, \phi_i), H(r_i, \phi_i)] = 0,$$
 (14)

where  $R[\ ]$  is the nonlinear operator representing (12). Since the deflection w is related to the spacing H through the head contour  $\overline{H}$ , Eqs. (13) and (14) can be directly combined to give

$$R\{P(r_i, \phi_i), L[P(r_i, \phi_i)] - \overline{H}(r_i, \phi_i)\} = 0.$$
 (15)

Equation (15) now has only one unknown (P) and can be solved by Gauss-Seidel relaxation in the same way that (12) was solved. This method still requires the solution of the elasticity equations through  $L[\ ]$ , but the need to solve the Reynolds equation during each iteration step is eliminated. Also, the relaxation factors can now be raised from approximately 0.01 with the old method to about 0.5 with this scheme. The result is to cut the computation time in half.

Other techniques have also proved effective. Subroutines have been written which detect oscillations and other potential problems in an attempt to optimize convergence. When oscillation is detected, the relaxation factor is automatically decreased. Local inaccuracies sometimes develop due to the calculation of spacing increments using fewer modes and grid points. If this condi-

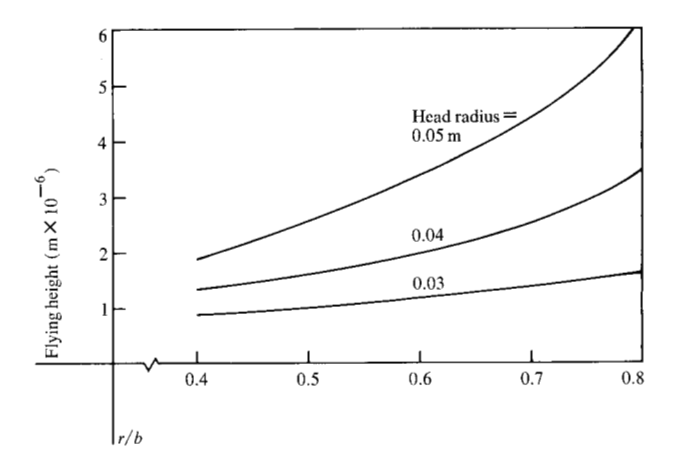


Figure 3 Flying height vs. radial head position for different values of the head radius.

tion is diagnosed, the number of modes and grid points during incremental calculations is automatically increased. If, during iteration, the disk is moving rapidly toward the head, then the relaxation factor is temporarily reduced in order to avoid a head crash. A good initial guess has been developed which also speeds the process. This initial guess is automatically scaled in order to begin with a reasonable value of the minimum spacing.

An attempt to further reduce computation time was made by using the incompressible Reynolds equation of lubrication. However, since the procedure developed here uses iteration, no additional time savings was realized by making this simplification. Furthermore, at close spacings the incompressible assumption would be less valid.

### Results and discussion

Using the procedure outlined, convergence time was reduced from ten hours to about thirty minutes. Solutions were obtained for all cases studied, including high-penetration configurations (although computation times were greater for such cases). Figure 3 shows the variation of flying height with radial head position for different values of the head radius. Note that even though the relative penetration increases with increased radius (an axisymmetric disk deflection is produced due to the presence of the base plate [7]), the flying height increases sharply. This is because the greater disk flexibility at larger values of the radius is more important than the difference in the relative penetration. Increased head radius generally corresponds to greater flying heights. This causes the pressure to be distributed over a larger area of the head and avoids the high pressure gradients near the head apex, resulting in the disk-to-head spacing being more nearly uniform. A similar effect is produced when the overall head dimen-

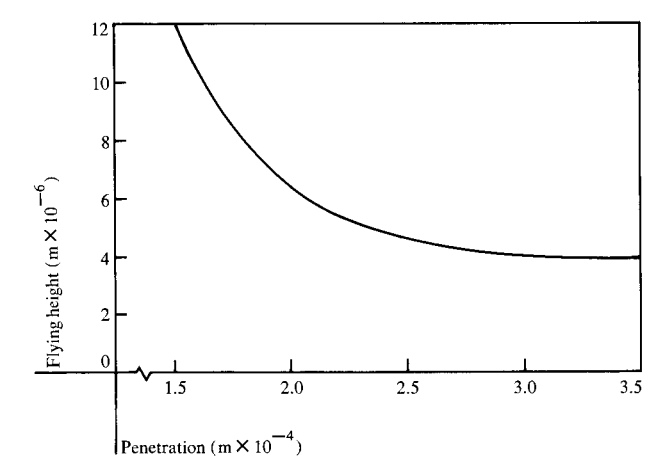
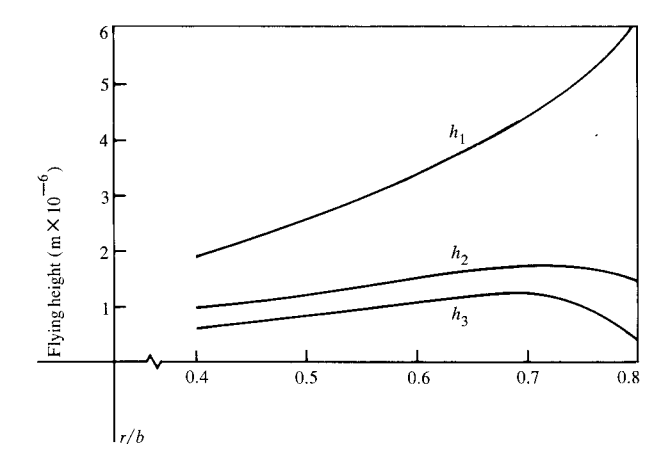


Figure 4 Flying height vs. head penetration.



**Figure 5** Flying height vs. radial head position for different disk thicknesses h, where  $h_1 < h_2 < h_3$ .

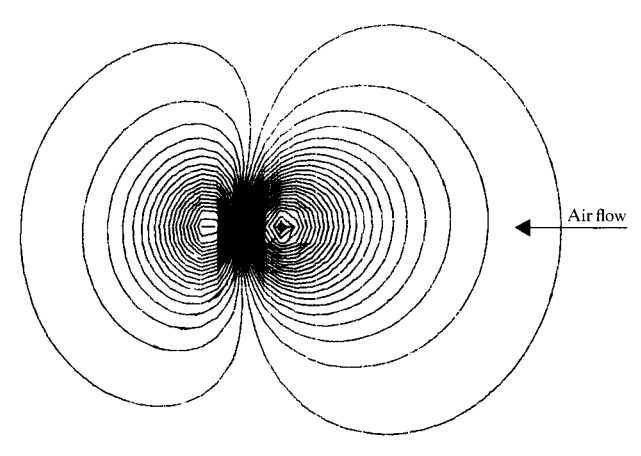


Figure 6 Pressure contours between disk and head.

sions are increased. The effect of head penetration on flying height is shown in Fig. 4. As could be expected, the flying height decreases with increased penetration but appears to level off as the penetration becomes large. This is because the disk tends to "wrap around" the head to a greater extent, thereby reducing the average value of the disk-to-head spacing but not changing its minimum value significantly. The location of the point of minimum spacing does shift somewhat in the downstream direction. The net force acting on the disk through the air bearing does increase with penetration, as do the corresponding pressures and pressure gradients. The most pronounced effect on flying height comes from the disk thickness (Fig. 5). This is because the disk stiffness varies as the cube of its thickness, requiring a much greater resultant force to act on the disk. The local bending of the disk becomes very small as the thickness increases. This also causes a very steep pressure gradient and a significantly lower minimum spacing near the head apex.

Pressure contours for a typical case are shown in Fig. 6. The results show positive pressures upstream and negative downstream with a steep pressure gradient near the head apex. The steepness of the pressure gradient is affected by head curvature, head dimensions, penetration, and disk thickness. The disk-to-head spacing contours shown in Fig. 7 are nearly circular. Although it is not at first obvious, these agree with the profile plots of Figs. 8 and 9. Note that the disk deflection is nearly symmetric in the radial direction, but very asymmetric circumferentially. This is due to the coupling of the disk dynamics with the lubrication theory as well as the foundation damping. As the disk thickness increases, the spacing contours are due principally to the head curvature, rather than to the local bending of the disk. Finally, Fig. 10 shows the disk deflection throughout the entire disk with the standing-wave pattern near the trailing edge. The presence of these waves indicates the importance of the dynamic effects included in the first term in (1). The results shown are in good qualitative agreement with experiments conducted using white-light interferometry.

#### **Acknowledgments**

The author thanks F. E. Talke, D. B. Bogy, N. A. Feliss, and H. J. Greenberg for their comments and discussions during the course of this research.

#### References

- 1. I. Pelech and A. H. Shapiro, "Flexible Disk Rotating on a Gas Film Next to a Wall," ASME J. Appl. Mech. 31, 577-584 (1964).
- R. C. Benson and D. B. Bogy, "Deflection of a Very Flexible Spinning Disk Due to a Stationary Transverse Load," ASME J. Appl. Mech. 45, 636-642 (1978).

G. G. ADAMS

516

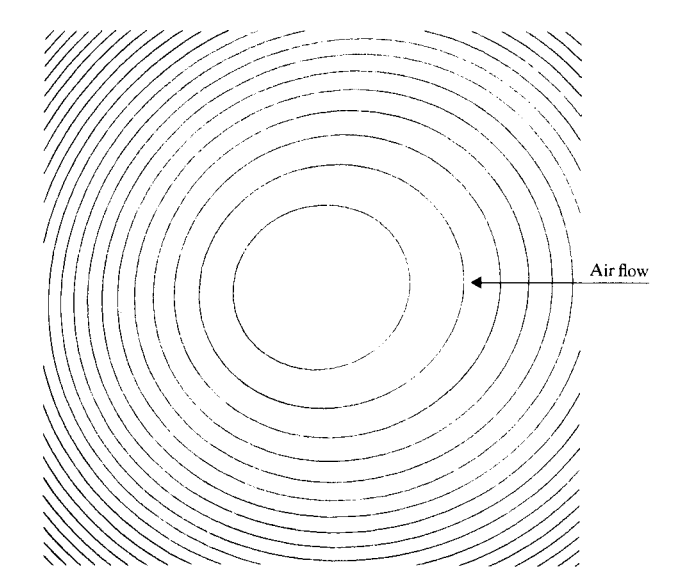
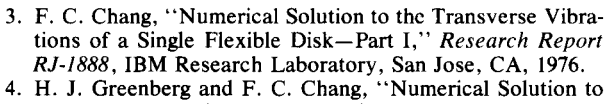
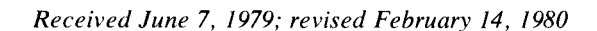


Figure 7 Spacing contours between disk and head.



- H. J. Greenberg and F. C. Chang, "Numerical Solution to the Transverse Vibrations of a Single Flexible Disk—Part II," Research Report RJ-2247, IBM Research Laboratory, San Jose, CA, 1978.
- H. J. Greenberg, "Flexible Disk—Read/Write Interface," IEEE Trans. Magnetics MAG-14, 336-338 (1978).
- H. J. Greenberg, "Study of Head-Tape Interaction in High Speed Rotating Head Recording," IBM J. Res. Develop. 23, 197-205 (1979).
- 7. G. G. Adams, "Analysis of the Flexible Disk/Head Interface," ASME J. Lubr. Technol. 102, 86-90 (1980).
- 8. L. Fox, The Numerical Solution of Two-Point Boundary Problems in Ordinary Differential Equations, Oxford University Press, London, 1957, Ch. 4.
- A. Burgdorfer, "The Influence of the Mean Free Path on the Performance of Hydrodynamic Gas Lubricated Bearings," ASME J. Basic Engineering 81D, 94-100 (1959).
- W. A. Michael, "A Gas Film Lubrication Study—Part II: Numerical Solution of the Reynolds Equation for Finite Slider Bearings," IBM J. Res. Develop. 3, 256-259 (1959).



The author is located at Northeastern University, Boston, Massachusetts; at the time this work was performed he held a postdoctoral position as a visiting scientist at the IBM Research Division laboratory, 5600 Cottle Road, San Jose, California 95193.

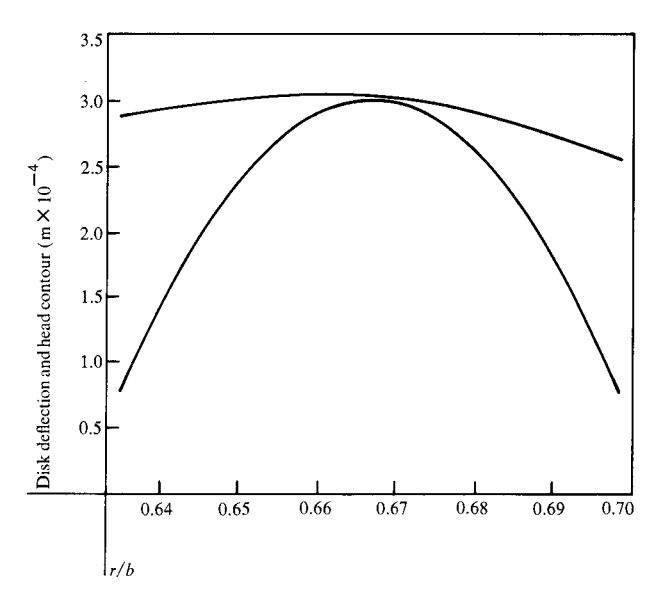


Figure 8 Profile of disk and head (radial direction).

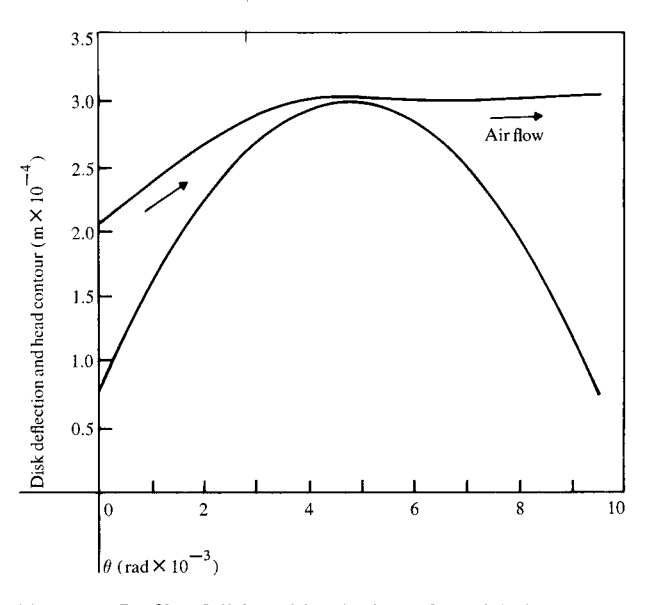


Figure 9 Profile of disk and head (circumferential direction).

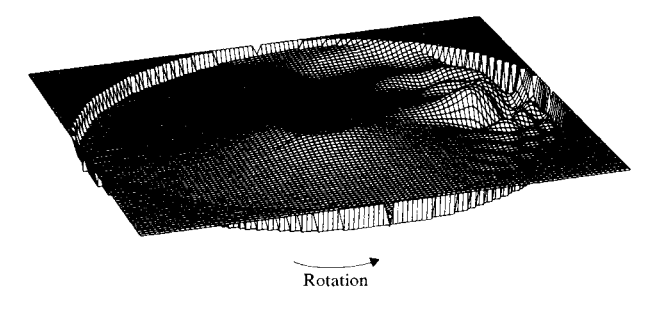


Figure 10 Disk deflections with standing-wave pattern (taken from Reference [7], copyright 1980 by the ASME; reprinted with permission).

517